



Published in final edited form as:

*Int J Cancer*. 2009 October 1; 125(7): 1595–1603. doi:10.1002/ijc.24479.

## LUNG CANCER SECRETED MICROVESICLES: UNDERAPPRECIATED MODULATORS OF MICROENVIRONMENT IN EXPANDING TUMORS

**Marcin WYSOCZYNSKI** and **Mariusz Z. RATAJCZAK\***

Stem Cell Biology Program at James Graham Brown Cancer Center, University of Louisville, Louisville, Kentucky, U.S.A and Department of Physiology Pomeranian Medical University, Szczecin, Poland

### Abstract

Microvesicles (MVs) are shed from cell membranes of several cell types and have an important function in cell-to-cell communication. Exponentially growing lung cancer cells secrete large quantities of MVs and we were interested in their role in tumor progression. We observed that both human and murine lung cancer cell lines secrete more MVs in response to non-apoptotic doses of hypoxia and irradiation. These tumor-derived (t)MVs activate and chemoattract stroma fibroblasts and endothelial cells. Furthermore, they induce expression of several pro-angiopoietic factors in stromal cells such as IL-8, VEGF, LIF, OSM, IL-11, and MMP-9. We also noticed that conditioned media harvested from stroma cells stimulated by tMVs enhanced the metastatic potential of both human and murine lung cancer cells *in vivo*. Thus, we postulated that tMVs are underappreciated constituents of the tumor microenvironment and play a pivotal role in tumor progression, metastasis, and angiogenesis.

### Keywords

lung cancer; tumor microvesicles; metastasis; angiogenesis; matrix metalloproteinases

### Introduction

There has been a recent focus on circular membrane fragments called microvesicles (MVs), which for many years have been largely overlooked. MVs are shed from the surface membranes of cells as well as secreted from the endosomal compartment as circular membrane fragments. They contain numerous proteins and lipids similar to those present in the membranes of the cells from which MVs originate. Furthermore, because they engulf some cytoplasm during membrane budding, they may also contain proteins and mRNA. Thus, MVs may stimulate target cells directly by surface-expressed ligands acting as a kind of “signaling complex”<sup>1, 2</sup>.

It had been postulated that this MV-mediated cell-to-cell communication system emerged very early in evolution and served as a template for the development of cell-to-cell interaction mechanisms involving soluble bioactive mediators and fine-tuned ligand-receptor interactions. In addition, MVs may transfer surface receptors from one cell to another and deliver proteins, mRNA, bioactive lipids, and even whole organelles (e.g.,

\*Correspondence to: Mariusz Z. Ratajczak MD, PhD Hoenig Endowed Chair in Cancer Biology Professor and Director of Stem Cell Institute University of Louisville 500 South Floyd Street Louisville, KY 40202, Kentucky, USA Tel: (502) 852-1788 Fax: (502) 852-3032 mzrata01@louisville.edu.

mitochondria) and infectious particles (e.g., HIV or prions) into target cells 3<sup>-8</sup>. In support of this, we recently demonstrated that peripheral blood (PB) platelet-derived (P)MV<sub>s</sub> promote the growth and metastatic potential of human lung and breast cancer cells by directly stimulating cancer cells as well as by transferring platelet-derived adhesion molecules to their surfaces 9<sup>-10</sup>.

The microenvironment of the growing tumor is enriched in MVs secreted not only by activated platelets and tumor infiltrating cells (e.g., monocytes, lymphocytes) but also by cancer cells themselves. All these MVs create a basis for a network of intercellular interactions that modulate tumor expansion and metastasis 10<sup>-15</sup>. In this study, we were interested in determining whether tumor-derived (t)MV<sub>s</sub> affect the biology of major cellular components of growing tumors (endothelial cells and stroma fibroblasts). As a model, we employed MVs secreted by human and murine lung cancer cell lines. Here, we provide evidence indicating that tMV<sub>s</sub> actively modulate the behavior of endothelium and tumor stroma. Based on this, we postulate that tMV<sub>s</sub> affect several biological processes that are important in tumor metastasis.

## Material and Methods

### Cell lines

Human lung cancer cell lines were obtained from the American Type Culture Collection (ATCC; Rockville, MD), specifically HTB 177 from large-cell lung cancers and CCL 185 (A549) from a highly metastatic human lung carcinoma. A murine cell line CRL 1642 (Lewis lung carcinoma, LLC) derived from C57BL mice was also purchased from ATCC. All cell lines were maintained in RPMI 1640 medium (Gibco BRL, Grand Island, NY) supplemented with 10% fetal bovine serum (FBS; Hyclone, Logan, UT).

### Evaluation of tMV production

Human and murine lung cancer cell lines were exposed to hypoxia (1% O<sub>2</sub>) or gamma irradiation (1000 cGy) and cultured for 12, 24, 36, or 48 hrs. The number of secreted tMV<sub>s</sub> was evaluated using flow cytometry by gating events smaller than 1µm. The cytometer-stopping gate was set up for 1000 events collected from the gate containing nucleated cells. The gating strategy is shown in Figure 1 panel C.

### Isolation of tMV<sub>s</sub>

Murine (LL-2) and human (A549 and HTB177) lung cancer cell lines were cultured in normal culture media (RPMI 1640 medium supplemented with 10% FBS). Culture media were collected every 48 hrs and centrifuged at 2000 RPMs for 30 min to remove cellular debris. Obtained supernatants were centrifuged at 20,000 RPM for 2 hrs. Pellets of tMV<sub>s</sub> were washed in cold phosphate-buffered saline (PBS) supplemented with 5mM HEPES.

### Preparation of bone marrow (BM) fibroblast-derived conditioned media (CM)

Human or murine BM fibroblasts were cultured in DMEM (Gibco BRL) supplemented with 10% FBS (Hyclone) until 80% confluence. At that point, fibroblasts were washed in PBS and culture media were replaced by serum-free media [0.5% of bovine serum albumin (BSA) in DMEM] or serum-free media supplemented with tMV<sub>s</sub> (50µg/ml). Twenty-four hours later, all media were collected and centrifuged at 20,000 RPM for 2 hrs at 4°C to remove cellular debris and MVs were employed for stimulation. CM were subsequently stored at -80°C until used in experiments.

## Phosphorylation of intracellular pathway proteins

Western blot analysis was performed on protein extracts from BM fibroblasts cells after stimulation with tMVs (50 µg/mL) for 10 min at 37°C. Phosphorylation of serine/threonine kinase AKT and p44/42 mitogen-activated protein kinase (MAPK) was detected by protein immunoblotting using mouse monoclonal 44/42 phospho-specific MAPK antibody and rabbit phospho-specific polyclonal antibodies (all from New England Biolabs, Beverly, MA) for each of the remainder. Horseradish peroxidase (HRP)-conjugated goat anti-mouse immunoglobulin (Ig)G or goat anti-rabbit IgG (Santa Cruz Biotechnology, Santa Cruz, CA) was used as a secondary antibody, as described. Equal loading in the lanes was evaluated by stripping the blots using IgG elution buffer (Pierce, Rockford, IL) according to the manufacturer's protocol. Briefly, membranes were washed overnight in IgG elution buffer at room temperature (RT), then washed in Tris-Tween-buffered saline (TTBS) and reprobed with appropriate monoclonal or polyclonal antibodies: p42/44 anti-MAPK antibody clone 9102 and anti-AKT antibody clone 9272 (Santa Cruz Biotechnology). The membranes were developed with an ECL reagent (Amersham Life Sciences, Little Chalfont, UK), dried, and exposed to film (HyperFilm, Amersham).

## In vivo matrigel assay

Angiogenesis assays were carried out by implanting subcutaneously 0.5 mL Matrigel implants (BD Biosciences Pharmingen, San Diego, CA) mixed on ice with 100 µg of A549-derived MVs or no MVs (controls) into severe combined immunodeficient (SCID) mice. Matrigel implants were injected subcutaneously in the abdominal midline on day 0 and subsequently isolated after four weeks. The level of vascularization was evaluated by determination of hemoglobin content using the Drabkin method. Briefly, the Matrigel implants were harvested and all surrounding tissues were dissected away. Cell pellets were homogenized at 4°C and assayed for hemoglobin content according to the manufacturer's protocol (Drabkin's reagent kit; Sigma Diagnostics, St. Louis, MO).

## Chemotaxis assay

Human umbilical vein endothelial cells (HUVECs) were resuspended in RPMI with 0.5% BSA (Sigma) and equilibrated for 10 min at 37°C. Pre-warmed serum-free medium containing tMVs or PMVs (50 µg/mL) was added to the lower chambers of a Costar Transwell 24-well plate (Costar Corning, Cambridge, MA). Cells were seeded into the upper chambers at a density of  $1 \times 10^5$  in 100 µL. After 24 hrs, the cells that had transmigrated were counted either on the lower side of the membrane or on the bottom of the transwell. The results are presented as a migration index (the ratio of the number of cells migrating toward the medium containing tMVs or PMV to the number of cells migrating toward the medium alone).

## Adhesion to HUVECs

Murine LL-2 and human A549 cells were labeled before assay with the fluorescent dye calcein-AM for 30 min in serum-free media. Next, cells were incubated with control media, CM from fibroblasts, and CM harvested from fibroblast stimulated with MVs then added for 15 min ( $10^5$  cells/well) to the 96-well plates covered by HUVECs that had been pretreated for 16 hrs with tumor necrosis factor (TNF)-alpha (5ng/mL). After the nonadherent cells had been discarded, the cells that adhered to the HUVECs were evaluated with using a fluorescent microscope.

## Cell proliferation assay

HUVECs were cultured in serum-free medium supplemented with 0.5% BSA in the presence of tMVs (50 µg/mL) for 72 hrs. Cells were cultured in 96-well plates at a

concentration of  $0.2 \times 10^5$  per well at  $37^\circ\text{C}$  in a fully humidified atmosphere supplemented with 5%  $\text{CO}_2$ . The number of cells was evaluated in a hemacytometer chamber.

### Real time PCR

For analysis of mRNA levels of Interleukin (IL)-1, IL-6, IL-8, IL-11, vascular endothelial growth factor (VEGF), hepatocyte growth factor (HGF), stromal cell-derived factor-1 (SDF-1), leukemia inhibitory factor (LIF), oncostatin M (OSM), matrix metalloproteinase (MMP)-2, MMP-9, tissue inhibitor of metalloproteinases (TIMP)-1, and TIMP-2, total mRNA was isolated from cells with the RNeasy Mini Kit (Qiagen, Valencia, CA). The mRNA was reverse-transcribed with TaqMan Reverse Transcription Reagents (Applied Biosystems, Foster City, CA) as described. Detection of IL-1, IL-6, IL-8, IL-11, VEGF, HGF, SDF-1, LIF, OSM, MMP-2, MMP-9, TIMP-1, TIMP-2, and  $\beta$ 2-microglobulin mRNA levels was performed by real-time reverse transcriptase-polymerase chain reaction (RT-PCR) using an ABI PRISM® 7000 Sequence Detection System (Applied Biosystems). A 25  $\mu\text{L}$  reaction mixture contained 12.5  $\mu\text{L}$  SYBR Green PCR Master Mix and 10 ng of cDNA template (Table I). Primers were designed with Primer Express software. The threshold cycle (Ct), i.e., the cycle number at which the amount of amplified gene of interest reached a fixed threshold, was subsequently determined. Relative quantitation of mRNA expression for IL-1, IL-6, IL-8, IL-11, VEGF, HGF, SDF-1, LIF, OSM, MMP-2, MMP-9, TIMP-1, and TIMP-2 was calculated with the comparative Ct method. The relative quantitation value of target, normalized to an endogenous control- $\beta$ 2-microglobulin gene and relative to a calibrator, is expressed as  $2^{-\Delta\text{Ct}}$  (fold difference), where  $\Delta\text{Ct} = \text{Ct of target genes (IL-1, IL-6, IL-8, IL-11, VEGF, HGF, SDF-1, LIF, OSM, MMP-2, MMP-9, TIMP-1, and TIMP-2)} - \text{Ct of the endogenous control gene } (\beta\text{-microglobulin})$  and  $\text{Ct} = \text{Ct of samples for target gene} - \text{Ct of the calibrator for the target gene}$ .

### Flow cytometry

The expression of intercellular adhesion molecule (ICAM), vascular cell adhesion molecule (VCAM), and CD49f protein was evaluated by fluorescence-activated cell sorter (FACS). The ICAM and VCAM antigens were detected with purified specific monoclonal antibodies and secondary fluorescein isothiocyanate (FITC)-conjugated antibody. CD49f antigen was detected using phycoerythrin (PE)-directly conjugated monoclonal antibody. Samples stained with appropriate isotype controls (all from BD Pharmingen) were examined in parallel.

### In vivo model of metastasis of murine LLC

Five- to 6-week-old male C57BL/6 mice (National Cancer Institute, Bethesda, MD) were injected intravenously with  $10^5$  LLC cells that had been incubated with CM collected from murine BM stromal cell cultures, stromal cells stimulated with LLC-derived MVs, or not with serum-free media. Incubation was performed for 60 min at  $37^\circ\text{C}$ . Before injection, cells were washed in PBS. After 2–3 weeks, the mice were sacrificed; their lungs were collected and fixed in ethanol. The number of metastatic foci was scored in the organs using a magnifying glass.

### In vivo model of metastasis of human A549 cells

Five- to 6-week-old male SCID-Beige inbred mice (National Cancer Institute) were injected intravenously with  $5 \times 10^6$  A549 cells that had been incubated with CM collected from human BM stromal cell cultures, stromal cells stimulated with A549-derived MVs, or not with serum-free media. Incubation was performed for 60 min at  $37^\circ\text{C}$ . Before injection, cells were washed in PBS. After 48 hrs, the mice were killed and their lungs were collected. Presence of A549 cells (i.e., murine-human chimerism) was evaluated as the difference in the level of human-satellite. DNA was amplified in the extracts isolated from the BM-

derived- and the lung-derived cells, using real-time PCR. Briefly, DNA was isolated using the QIAamp DNA Mini kit (Qiagen). Detection of human-satellite and murine  $\beta$ -actin DNA levels was accomplished using real-time PCR and an ABI Prism 7000 Sequence Detection System. A 25- $\mu$ L reaction mixture contained 12.5  $\mu$ L SYBR Green PCR Master Mix, 300 ng DNA template, 5'-GGG ATA ATT TCA GCT GAC TAA ACA G-3', 5'-TTT CGT TTA GTT AGG TGC AGT TAT C-3', and 5'-AAA CGT CCA CTT GCA GAT TCT AG-3' primers for the -satellite and 5'-GGA TGC AGA AGG AGA TCA CTG-3' forward and 5'-CGA TCC ACA CGG AGT ACT TG-3' reverse primers for the  $\beta$ -actin. Ct was determined as before. The number of human cells present in the murine lungs (degree of chimerism) was calculated from the standard curve obtained by mixing different numbers of human cells with a constant number of murine cells.

### Statistical Analysis

All results are presented as mean  $\pm$  standard error (SEM). Statistical analysis of the data was performed using the nonparametric Mann-Whitney test with  $p < 0.05$  considered significant.

## Results

### Lung cancer cells secrete MVs in response to hypoxia and irradiation

It had been reported that growing tumor cell lines (e.g., lung cancer cells) secrete MVs into the culture media<sup>15</sup>. Thus, we were interested in determining whether factors that influence tumor growth such as hypoxia or  $\gamma$ -irradiation would increase MV secretion by lung cancer cells. To address this question, murine LL-2 and human A549 cells were exposed to hypoxia (1% O<sub>2</sub>) for 12–48 hrs. CM harvested from these cells were evaluated for a presence of MVs by FACS. Figure 1 panel A shows that cells cultured in hypoxic conditions secreted up to 4 times more MVs as compared to cells cultured in standard conditions. Similarly, Figure 1 panel B shows that LL-2 and A549 cells secreted up to 4 times more MVs after exposure to  $\gamma$ -irradiation (1000cGy), as measured 12–48 hrs after irradiation. Of note, the doses of irradiation employed did not affect the viability of LL-2 and A549 cells as assayed 48 hrs later by 0.5% trypan blue exclusion test (Supplementary Figure 1).

Because secretion of MVs by platelets depends on lipid rafts, we asked whether MV secretion by tumor cells would be inhibited if we depleted the cell membranes from a major component of lipid rafts, that of cholesterol<sup>16</sup>. In fact, we found that pre-incubation of A549 cells with methyl- $\beta$ -cyclodextran (1mM – 5mM) for 30 min reduced secretion of MVs by 40% (Supplementary Figure 2). Thus, these data show that tumor cells may increase or decrease secretion of MVs in response to micro-environmental changes.

### Lung cancer cell-derived MVs stimulate and chemoattract endothelial cells

To expand in size, growing tumors need to chemoattract endothelial cells. We asked whether lung cancer cell line-derived MVs might interact with endothelial cells. However, A549- and LL-2 cell-derived tMV<sub>s</sub> (50 $\mu$ g/ml) did not influence proliferation of HUVECs (data not shown). Both murine LL-2- and human A549-derived tMV<sub>s</sub> induced phosphorylation of MAPKp42/44 and AKT in these cells (Figure 2 panel A) similarly to PMVs.

More importantly, we noticed that both LL-2- and A549 tMV<sub>s</sub> also strongly chemoattract HUVECs (Figure 2 panel B) similarly to PMVs. Furthermore, tMV<sub>s</sub> significantly increased vascularization in matrigels implanted subcutaneously into immunodeficient mice, as evaluated by hemoglobin level using Drabkin assay (Figure 2 panel C). We also noticed that stimulation of HUVECs with A549-derived tMV<sub>s</sub> upregulated expression of mRNA for IL-8, VCAM, and ICAM but not von Willebrand factor (vWF) and lymphocyte function-associated antigen-1 (LFA-1) in HUVECs (Figure 2 panel D), which was subsequently



confirmed by employing enzyme-linked immunosorbent assay (ELISA; for IL-8) and FACS (for ICAM, VCAM) at the protein level (Figure 2 panels E and F, respectively). Together, these data indicate that lung cancer-derived tMVs play an underappreciated role in regulating the biology of the endothelium.

### **Lung cancer cell-derived tMVs stimulate stroma fibroblasts**

As described above, in similar sets of experiments, we found that lung cancer tMVs do not stimulate proliferation of BM- or lung-derived fibroblasts (data not shown). However, exposure of murine and human BM-derived fibroblasts as well as murine lung-derived fibroblasts to lung cancer tMVs stimulated phosphorylation of MAPKp42/44 and AKT (Figure 3 panels A, B, and C, respectively).

Because fibroblasts are a source of several factors that may modulate tumor growth, in the next step, we evaluated the effect of tMV stimulation on expression of several factors that may modulate tumor expansion. As shown in Table I, murine and human lung cancer tMVs stimulated in BM and lung isolated fibroblast expression of several factors involved in tumor expansion similarly to PMVs. Accordingly, tMVs stimulated expression of pro-angiopoietic factors such as IL-8, VEGF, LIF, OSM, and IL-11 as well as expression of MMP-9. Interestingly, heat inactivation of MVs before stimulation of fibroblasts decreased expression of mRNA for these factors, which suggests involvement of protein components of MVs to the observed phenomena (data not shown).

Finally, since we identified the expression of the mentioned pro-angiopoietic factors in fibroblasts stimulated by lung cancer tMVs, we tested whether CM harvested from fibroblasts may better chemoattract HUVECs. First, we found that HUVECs respond better by phosphorylation of MAPKp42/44 and AKT if exposed to CM harvested from BM-derived fibroblasts that were previously stimulated by lung cancer-derived tMVs (Figure 4 panel A). At the same time, these CM better chemoattracted HUVECs in a transwell migration assay (Figure 4 panel B). Based on this, tMVs secreted by both murine and human lung cancer cells may affect several processes in tumor-associated fibroblasts.

### **Stroma fibroblasts stimulated by tMVs stimulate both lung cancer cells and endothelial cells**

The data presented above demonstrate that tMVs secreted by lung cancer cells may directly stimulate endothelial cells and fibroblasts that are crucial components of expanding tumors. Thus, we sought to determine whether stroma cells stimulated by tMVs might also affect lung cancer cells.

To address this issue, we exposed murine LL-2 cells to CM harvested from murine lung-derived fibroblasts stimulated or non-stimulated by LL-2-derived tMVs. Figure 5 panel A shows that lung fibroblasts stimulated by tMVs secrete some factors that in turn activate phosphorylation of STAT3, AKT, and MAPKp42/44 in LL-2 cells. We also noticed that CM harvested from murine fibroblasts exposed to LL-2 tMVs not only better chemoattracted murine LL-2 cells, but more importantly they: i) “sensitize” chemotactic responses of LL-2 cells to factors secreted by BM fibroblasts; and ii) simultaneously increase adhesion of LL-2 cells to HUVECs (Figure 5 panels B and C).

### **Stroma fibroblasts stimulated by tMVs enhance metastatic potential of lung cancer cells**

Finally, to test whether LL-2 and A549 cells show increased metastasis when incubated with CM harvested from fibroblasts stimulated with LL-2- or A549-derived tMVs, respectively, we performed *in vivo* metastatic assays. Accordingly, LL-2 and A549 cells pre-stimulated with CM from fibroblasts exposed or non-exposed to tMVs were injected intravenously

(Figure 5 panels D and E). Forty-eight hours later, we evaluated a number of A549 cells present in lungs of immunodeficient mice and a number of metastases visible on lungs of C57Bl6 mice 2–3 weeks after LL-2 cell infusion. We noticed that stimulation of lung cancer cells by CM from stroma cells stimulated by tMVs enhances *in vivo* metastatic potential of both human (Figure 5 panel D) and murine (Figure 5 panel E) lung cancer cells.

Together, these data show involvement of tMVs in crosstalk between tumor cells and the microenvironment, but also for the first time reveal a presence of feedback signals that tumor cells receive from stroma fibroblasts that are stimulated by the tMVs that they secrete.

## Discussion

Cells communicate and exchange information by employing different mechanisms such as secreted soluble factors or cell-to-cell adhesion contacts. However, attention is now being focused on cell-to-cell communication that involves MVs, a mechanism that for many years has been largely overlooked. Shedding of membrane-derived MVs is a physiological phenomenon that accompanies cell activation and growth. MVs may: i) stimulate other cells by surface-expressed ligands acting as a “signaling complex”; ii) transfer surface receptors from one cell to another; and iii) as we reported recently, even deliver proteins, mRNA, and bioactive lipids into the target cells<sup>17–21</sup>.

Evidence accumulates that MVs are important constituents of the tumor microenvironment and are secreted by platelets (PMVs), tumor infiltrating leucocytes, and, more importantly, the expanding tumor cells themselves, which secrete tMVs<sup>9–15</sup> (Figure 6). Considerable progress has been made in recognizing MVs as important mediators of intercellular communication rather than irrelevant cell debris. In our previous study, we demonstrated that human and murine lung cancer cell lines activate platelets. We also showed that PMVs modulate metastatic potential of lung cancer cells by directly stimulating cancer cells and by transferring platelet-derived integrins to the membranes of those cancer cells that may efficiently facilitate interaction with the endothelium. As such, this enhances metastasis of cancer cells circulating in the PB10.

In the current study, we provide evidence that growing lung cancer cells secrete MVs and that the number of these lung cancer-derived tMVs increases in response to hypoxia and gamma irradiation at doses that do not affect cell viability. This would support the hypothesis that MVs secretion is related to cellular stress and MVs are distinct from apoptotic bodies.

We also noticed that tMVs directly chemoattract endothelial cells and activate phosphorylation of MAPKp42/44 and AKT. Moreover, endothelial cells stimulated by tMVs secrete more IL-8 and increase expression of ICAM and VCAM. This fact, in connection with increased secretion of tMVs during hypoxia, provides evidence that pro-angiopoietic tMVs should be considered as one of the cancer-derived factors that is responsible for tumor neo-vascularization. Thus, a more complex network of mutual pro-angiopoietic interactions emerges in which tMVs in addition to angiopoietic factors secreted during hypoxia by tumor cells (e.g., VEGF, IL-8) are playing an important and underappreciated role. To support this further, our Matrigel implants assay revealed that tMVs possess proangiopoietic activity *in vivo* as well.

Our data also indicate that tMVs may increase angiogenesis indirectly by activating stroma cells. Accordingly, we provide evidence that tMVs induce expression of several pro-angiopoietic factors in stromal cells such as IL-8, VEGF, LIF, OSM, IL-11, and MMP-9. Based on this, the presence of pro-angiopoietic tMVs in the tumor microenvironment should be considered while developing more effective antiangiopoietic therapeutics. Because the

production of MVs depends on the formation of membrane lipid rafts, it is possible that inhibitors of membrane lipid raft formation (e.g., statins or polyene antibiotics) could reduce MV formation<sup>16, 22, 23</sup>. This could explain some of the reported beneficial effects of statins on tumor growth/expansion. Further, since calcium flux is crucial for vesiculation, calcium blockers could potentially inhibit MV formation. Finally, a similar inhibitory effect on MV formation has been described after high dose Vitamin C therapy<sup>24–26</sup>.

Herein, we also deciphered another important aspect of tMV-mediated crosstalk with the tumor-supporting cells present in its microenvironment. Namely, we noticed that CM harvested from stroma cells, if stimulated by tMVs, might enhance the metastatic potential of both human and murine lung cancer cells. Accordingly, both human and murine lung cancer cells exposed to CM harvested from stroma cells exposed to tMVs show enhanced motility and more important higher metastatic potential in *in vivo* models. This suggests that some of the factors secreted by stroma cells may enhance the metastatic potential of lung cancer cells. Our initial observations indicate that these factors are heat inactivation-sensitive, which indicates that they could possess a protein/peptide structure. Further work is needed to identify such factor/s.

It is well known from the literature that the numbers of circulating MVs are increased in the PB of cancer patients and have been correlated in gastric cancer patients with increased metastasis and a worse prognosis, for example<sup>27</sup>. Our work lends support to these clinical observations and provides further evidence that tMVs are underappreciated constituents of the tumor microenvironment having a pivotal role in tumor progression, metastasis, and angiogenesis. These effects are explainable by activation/stimulation of endothelial and stromal cells. However, tMVs may also interact with other types of cells present in the tumor microenvironment. For example, a recent study demonstrated a beneficial effect of tMVs in increasing the survival of tumor-infiltrating monocytes. Accordingly, tMVs can transfer various surface determinants (e.g., CCR6 and CD44v7/8) to monocytes, exert an antiapoptotic effect on them, and activate AKT kinase (Protein Kinase B)<sup>28</sup>. With evidence accumulating that tMVs may paradoxically play a role in enhancing tumor vascularization, this would be another effect of tMVs in promoting tumor vascularization and growth.

In conclusion, the tumor microenvironment is highly enriched in MVs that are shed from cancer cells, activated blood platelets, and infiltrating the tumor tissue monocytes and lymphocytes (Figure 6). Evidence from our previous and current work supports that all these MVs orchestrate and are important mediators of tumor growth, progression, angiogenesis, and metastasis. However, further studies are needed to better understand the molecular mechanisms responsible for the biological effects of tMVs and to develop strategies to control their biological effects by developing new anti-MVs drugs (e.g., statin-based?). It is also worth evaluating whether tMVs possess some unique molecular signatures depending on their tumor origin that could be applicable in diagnostics.

Finally, it will be important to identify protein and lipid components of tMVs that are responsible for particular biological effects. In addition and as we demonstrated, because MVs transfer mRNA between cells<sup>2</sup>, tMVs should be analyzed for mRNA and micro-RNA content as well.

## Supplementary Material

Refer to Web version on PubMed Central for supplementary material.



## Acknowledgments

**GRANT SUPPORT:** Supported by NIH grant R01 CA106281-01 and the Stella & Henry Hoenig endowment to MZR.

## Abbreviations

|               |   |
|---------------|---|
| <b>ATCC</b>   | (American Type Culture Collection)                |
| <b>BM</b>     | (bone marrow)                                     |
| <b>BSA</b>    | (bovine serum albumin)                            |
| <b>CM</b>     | (conditioned media)                               |
| <b>Ct</b>     | (threshold cycle)                                 |
| <b>ELISA</b>  | (enzyme-linked immunosorbent assay)               |
| <b>FACS</b>   | (fluorescence-activated cell sorter)              |
| <b>FBS</b>    | (fetal bovine serum)                              |
| <b>FITC</b>   | (fluorescein isothiocyanate)                      |
| <b>HGF</b>    | (hepatocyte growth factor)                        |
| <b>HRP</b>    | (horseradish peroxidase)                          |
| <b>HUVEC</b>  | (human umbilical vein endothelial cell)           |
| <b>ICAM</b>   | (intercellular adhesion molecule)                 |
| <b>Ig</b>     | (immunoglobulin)                                  |
| <b>IL</b>     | (interleukin)                                     |
| <b>LFA-1</b>  | (lymphocyte function-associated antigen-1)        |
| <b>LIF</b>    | (leukemia inhibitory factor)                      |
| <b>LLC</b>    | (Lewis lung carcinoma)                            |
| <b>MAPK</b>   | (mitogen-activated protein kinase)                |
| <b>MMP</b>    | (matrix metalloproteinase)                        |
| <b>MV</b>     | (microvesicle)                                    |
| <b>OSM</b>    | (oncostatin M)                                    |
| <b>PB</b>     | (peripheral blood)                                |
| <b>PBS</b>    | (phosphate-buffered saline)                       |
| <b>PE</b>     | (phycoerythrin)                                   |
| <b>PMV</b>    | (platelet-derived microvesicle)                   |
| <b>RT</b>     | (room temperature)                                |
| <b>RT-PCR</b> | (reverse transcriptase-polymerase chain reaction) |
| <b>SCID</b>   | (severe combined immunodeficient)                 |
| <b>SDF-1</b>  | (stromal cell-derived factor- 1)                  |
| <b>SEM</b>    | (mean $\pm$ standard error)                       |
| <b>TIMP</b>   | (tissue inhibitor of metalloproteinase)           |

|             |                                      |
|-------------|--------------------------------------|
| <b>tMV</b>  | (tumor-derived microvesicle)         |
| <b>TNF</b>  | (tumor necrosis factor)              |
| <b>TTBS</b> | (Tris-Tween-buffered saline)         |
| <b>VCAM</b> | (vascular cell adhesion molecule)    |
| <b>VEGF</b> | (vascular endothelial growth factor) |
| <b>vWF</b>  | (von Willebrand factor)              |

## Literature

1. Baj-Krzyworzeka M, Szatanek R, Weglarczyk K, Baran J, Urbanowicz B, Branski P, Ratajczak MZ, Zembala M. Tumour-derived microvesicles carry several surface determinants and mRNA of tumour cells and transfer some of these determinants to monocytes. *Cancer Immunology & Immunotherapy*. 2006; 55:808–18. [PubMed: 16283305]
2. Ratajczak J, Miekus K, Kucia M, Zhang J, Reca R, Dvorak P, Ratajczak MZ. Embryonic stem cell-derived microvesicles reprogram hematopoietic progenitors: evidence for horizontal transfer of mRNA and protein delivery. *Leukemia*. 2006; 20:847–56. [PubMed: 16453000]
3. Fevrier B, Vilette D, Laude H, Raposo G. Exosomes: a bubble ride for prions? *Traffic*. 2005; 6:10–7. [PubMed: 15569241]
4. Pelchen-Matthews A, Raposo G, Marsh M. Endosomes, exosomes and Trojan viruses. *Trends in Microbiology*. 2004; 12:310–6. [PubMed: 15223058]
5. Robertson C, Booth SA, Beniac DR, Coulthart MB, Booth TF, McNicol A. Cellular prion protein is released on exosomes from activated platelets. *Blood*. 2006; 107:3907–11. [PubMed: 16434486]
6. Rozmyslowicz T, Majka M, Kijowski J, Murphy SL, Conover DO, Poncz M, Ratajczak J, Gaulton GN, Ratajczak MZ. Platelet- and megakaryocyte-derived microparticles transfer CXCR4 receptor to CXCR4-null cells and make them susceptible to infection by X4-HIV. *AIDS*. 2003; 17:33–42. [PubMed: 12478067]
7. Spees JL, Olson SD, Whitney MJ, Prockop DJ. Mitochondrial transfer between cells can rescue aerobic respiration. *Proceedings of the National Academy of Sciences of the United States of America*. 2006; 103:1283–8. [PubMed: 16432190]
8. Ratajczak J, Wysoczynski M, Hayek F, Janowska-Wieczorek A, Ratajczak MZ. Membrane-derived microvesicles: important and underappreciated mediators of cell-to-cell communication. *Leukemia*. 2006; 20:1487–95. [PubMed: 16791265]
9. Janowska-Wieczorek A, Marquez-Curtis LA, Wysoczynski M, Ratajczak MZ. Enhancing effect of platelet-derived microvesicles on the invasive potential of breast cancer cells. *Transfusion*. 2006; 46:1199–209. [PubMed: 16836568]
10. Janowska-Wieczorek A, Wysoczynski M, Kijowski J, Marquez-Curtis L, Machalinski B, Ratajczak J, Ratajczak MZ. Microvesicles derived from activated platelets induce metastasis and angiogenesis in lung cancer. *International Journal of Cancer*. 2005; 113:752–60.
11. Kanazawa S, Nomura S, Kuwana M, Muramatsu M, Yamaguchi K, Fukuhara S. Monocyte-derived microparticles may be a sign of vascular complication in patients with lung cancer. *Lung Cancer*. 2003; 39:145–9. [PubMed: 12581566]
12. Wolf P. The nature and significance of platelet products in human plasma. *British Journal of Haematology*. 1967; 13:269–88. [PubMed: 6025241]
13. Ginestra A, Miceli D, Dolo V, Romano FM, Vittorelli ML. Membrane vesicles in ovarian cancer fluids: a new potential marker. *Anticancer Research*. 1999; 19:3439–45. [PubMed: 10629632]
14. Kim CW, Lee HM, Lee TH, Kang C, Kleinman HK, Gho YS. Extracellular membrane vesicles from tumor cells promote angiogenesis via sphingomyelin. *Cancer Research*. 2002; 62:6312–7. [PubMed: 12414662]

15. Beaudoin AR, Grondin G. Shedding of vesicular material from the cell surface of eukaryotic cells: different cellular phenomena. *Biochimica et Biophysica Acta*. 1991; 1071:203–19. [PubMed: 1958687]
16. Del Conde I, Shrimpton CN, Thiagarajan P, Lopez JA. Tissue-factor-bearing microvesicles arise from lipid rafts and fuse with activated platelets to initiate coagulation. *Blood*. 2005; 106:1604–11. [PubMed: 15741221]
17. Rustom A, Saffrich R, Markovic I, Walther P, Gerdes HH. Nanotubular highways for intercellular organelle transport. *Science*. 2004; 303:1007–10. [PubMed: 14963329]
18. Vidulescu C, Clejan S, O'Connor KC. Vesicle traffic through intercellular bridges in DU 145 human prostate cancer cells. *Journal of Cellular and Molecular Medicine*. 2004; 8:388–96. [PubMed: 15491514]
19. Ponsaerts P, Berneman ZN. Modulation of cellular behavior by exogenous messenger RNA. *Leukemia*. 2006; 20:767–9. [PubMed: 16639419]
20. Haass NK, Herlyn M. Normal human melanocyte homeostasis as a paradigm for understanding melanoma. *The Journal of Investigative Dermatology*. 2005; 10:153–63. [PubMed: 16358819]
21. Morel O, Toti F, Hugel B, Freyssinet JM. Cellular microparticles: a disseminated storage pool of bioactive vascular effectors. *Current Opinion in Hematology*. 2004; 11:156–64. [PubMed: 15257014]
22. Lopez JA, del Conde I, Shrimpton CN. Receptors, rafts, and microvesicles in thrombosis and inflammation. *J Thromb Haemost*. 2005; 3:1737–44. [PubMed: 16102040]
23. Salzer U, Hinterdorfer P, Hunger U, Borken C, Prohaska R. Ca(++)- dependent vesicle release from erythrocytes involves stomatin-specific lipid rafts, synexin (annexin VII), and sorcin. *Blood*. 2002; 99:2569–77. [PubMed: 11895795]
24. Lee YJ, Jy W, Horstman LL, Janania J, Reyes Y, Kelley RE, Ahn YS. Elevated platelet microparticles in transient ischemic attacks, lacunar infarcts, and multiinfarct dementias. *Thrombosis Research*. 1993; 72:295–304. [PubMed: 8303669]
25. Rossig L, Hoffmann J, Hugel B, Mallat Z, Haase A, Freyssinet JM, Tedgui A, Aicher A, Zeiher AM, Dimmeler S. Vitamin C inhibits endothelial cell apoptosis in congestive heart failure. *Circulation*. 2001; 104:2182–7. [PubMed: 11684628]
26. Zhuang L, Kim J, Adam RM, Solomon KR, Freeman MR. Cholesterol targeting alters lipid raft composition and cell survival in prostate cancer cells and xenografts. *The Journal of Clinical Investigation*. 2005; 115:959–68. [PubMed: 15776112]
27. Kim HK, Song KS, Park YS, Kang YH, Lee YJ, Lee KR, Kim HK, Ryu KW, Bae JM, Kim S. Elevated levels of circulating platelet microparticles, VEGF, IL-6 and RANTES in patients with gastric cancer: possible role of a metastasis predictor. *Eur J Cancer*. 2003; 39:184–91. [PubMed: 12509950]
28. Baj-Krzyworzeka M, Szatanek R, Weglarczyk K, Baran J, Zembala M. Tumour-derived microvesicles modulate biological activity of human monocytes. *Immunology Letters*. 2007; 113:76–82. [PubMed: 17825925]

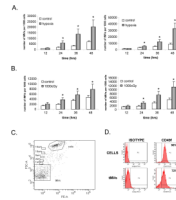


**Figure 1. Lung cancer cells secrete more MVs in response to hypoxia and gamma irradiation**  
**Panel A.** Murine LL-2 (left panel) and human A549 (right panel) cells were exposed to hypoxia (1% O<sub>2</sub>). The number of tMVs was evaluated by flow cytometry at 12, 24, 36, and 48 hrs after exposure to hypoxia. **Panel B.** Murine LL-2 (left panel) and human A549 (right panel) cells were exposed to gamma irradiation (1000cGy). Subsequently, 12, 24, 36, and 48 hrs later, the number of secreted MVs was evaluated by flow cytometry. **Panel C.** The gating strategy to evaluate tMV production in culture media. Size beads were used to establish the proper gate for events smaller than 1  $\mu$ m, which include tMVs. The stopping gate was set up on 1000 events collected from the tMV region. **Panel D.** A549 lung cancer cell-derived tMVs express CD49f similarly to parental cells. Data from four (panel A and B) or three (Panel C and D) separate experiments are pooled together. \* p<0.0001.

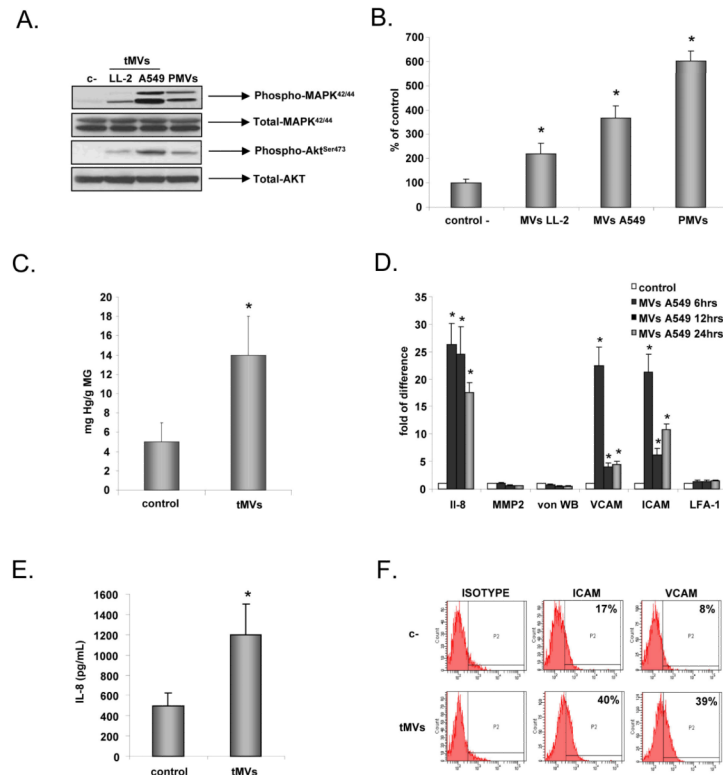


**Figure 2. Lung cancer cell-derived MVs stimulate and chemoattract endothelial cells**  
**Panel A.** Phosphorylation of MAPK p42/44 and AKT in HUVECs by LL-2 and A549 cell-derived tMVs. The experiment was repeated three times with similar results. A representative study is shown. **Panel B.** Chemotaxis of HUVECs to LL-2- and A549-derived tMVs and PMVs. HUVECs were resuspended in 0.5% BSA + RPMI and placed in the upper chambers of transwells. The lower transwell chambers contained medium supplemented with 50 $\mu$ g/mL of MVs. After 24 hrs, the cells attached to the lower portion of the transwell membrane were stained and counted under an inverted microscope. Data from four separate experiments are pooled together. \* $p < 0.0001$ . **Panel C.** Level of hemoglobin (Drabkin assay) in control (empty) and A549-derived MVs containing matrigels implanted for 4 weeks into SCID-Beige inbred mice. Data from three separate experiments are pooled together. \* $p < 0.0001$ . **Panel D.** HUVECs were stimulated with A549-derived tMVs (50 $\mu$ g/ml) for 6, 12, and 24 hrs. RNA was extracted to evaluate levels of mRNA for IL-8, MMP-2, vWF, VCAM, ICAM, and LFA-1 by real time PCR. Data from four separate experiments are pooled together. \* $p < 0.0001$ . **Panel E and F.** HUVECs were stimulated with A549-derived tMVs (50 $\mu$ g/ml) for 16 hrs. The level of IL-8 was evaluated in culture CM (Panel E) and expression of ICAM and VCAM on the HUVECs was evaluated by flow cytometry (Panel F). Data from three separate experiments are pooled together. \* $p < 0.0001$  for panel E. Panel F experiment was repeated three times with similar results and a representative study is shown.

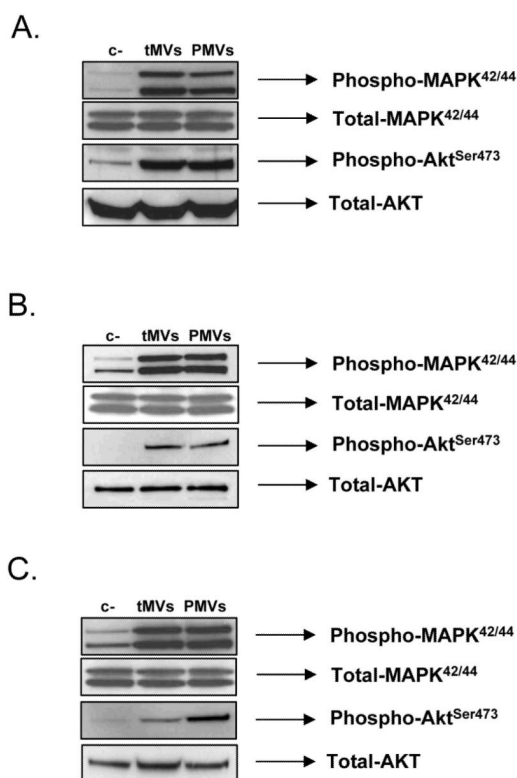


**Figure 3. Lung cancer cell-derived MVs stimulate phosphorylation of MAPK p42/44 and AKT in stroma fibroblasts**

**Panel A.** Stimulation of human stroma cells by A549 cell-derived tMVs. **Panel B.** Stimulation of human stroma cells by HTB177 cell-derived tMVs. **Panel C.** Stimulation of murine stroma cells by LL-2 cell-derived tMVs. The experiment was repeated three times with similar results. A representative study is shown.



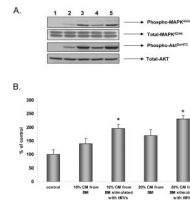


**Figure 4. CM from stroma cells exposed to MVs stimulate endothelial cells**

**Panel A.** Phosphorylation of MAPK p42/44 and AKT by CM harvested from control, unstimulated fibroblasts, and fibroblasts stimulated by tMVs. **Lane 1.** Unstimulated HUVECs. **Lane 2.** HUVECs stimulated for 10 min by 10% of CM from control fibroblasts. **Lane 3.** HUVECs stimulated for 10 min by 10% of CM from fibroblasts stimulated by tMVs. **Lane 4.** HUVECs stimulated for 10 min with 20% of CM from fibroblasts. **Lane 5.** HUVECs stimulated for 10 min with 20% of CM from fibroblasts stimulated with tMVs. The experiment was repeated three times with similar results. A representative study is shown. **Panel B.** HUVECs were resuspended in 0.5% BSA + RPMI and placed in the upper chambers of transwells. The lower transwell chambers contained 10% or 20% conditioned medium from fibroblasts or fibroblasts stimulated with tMVs. After 24 hrs, the cells attached to the bottom surface of the transwell membrane were stained and counted under an inverted microscope. Data from four separate experiments are pooled together. \* $p < 0.0001$ .

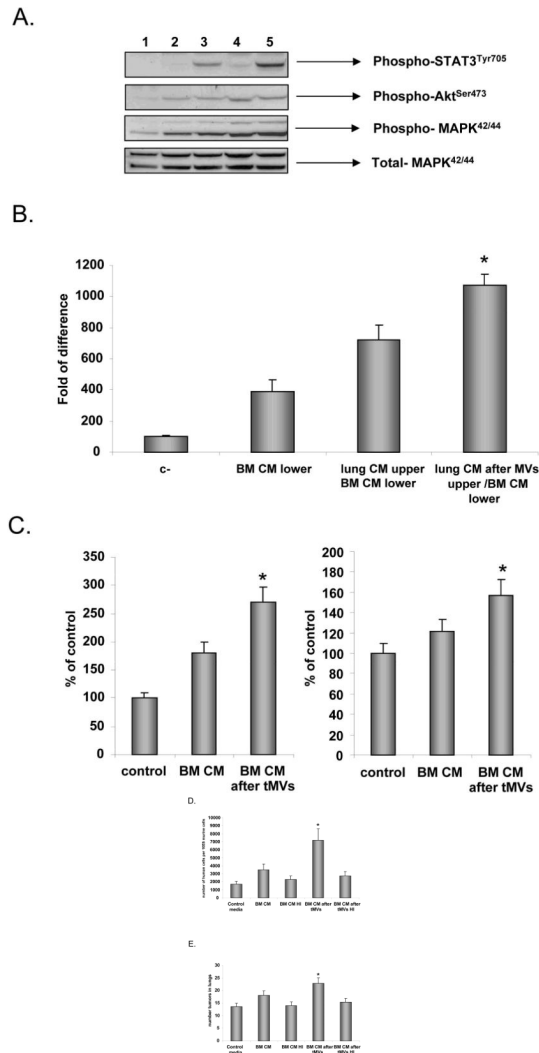


**Figure 5. CM from stroma cells stimulated with tMVs in turn stimulate cancer cells: the effect on signaling, chemotaxis, adhesion, and metastasis in vivo**  
**Panel A. Effect on signaling.** Phosphorylation of MAPK p42/44, AKT, and STAT3 by CM harvested from control, unstimulated fibroblasts, and fibroblasts stimulated with tMVs. **Lane 1.** Unstimulated LL-2 cells. **Lane 2.** Cells stimulated for 10 min with 10% of CM from fibroblasts. **Lane 3.** Cells stimulated for 10 min with 10% of CM from fibroblasts stimulated with LL-2-derived tMVs. **Lane 4.** Cells stimulated for 10 min with 20% of CM from fibroblasts. **Lane 5.** Cells stimulated for 10 min with 20% of CM from fibroblasts stimulated with LL2-derived tMVs. Data from four separate experiments are pooled together. \* $p < 0.0001$ . **Panel B. Effect on chemotaxis.** LL-2 cells were resuspended in 0.5% BSA + RPMI. CM from unstimulated lung fibroblasts or CM collected from lung fibroblasts stimulated with tMVs were placed in the upper chambers of transwells. The lower chambers contained medium supplemented with 10% of conditioned medium harvested from BM fibroblasts. After 24 hrs, the cells on the bottom surface of the transwell membrane were stained and counted under an inverted microscope. Data from four separate experiments are pooled together. \* $p < 0.0001$ . **Panel C. Effect on adhesion.** A549 cells (left part) and LL-2 cells (right graph) were incubated in control medium. The conditioned medium was collected from fibroblasts or fibroblasts stimulated with tMVs and added to a 96-well plate covered with HUVECs for 15 min. Floating cells were removed and adhered cells were

evaluated under microscope. Data from four separate experiments are pooled together. \* $p < 0.0001$ . **Panel D and E. Effect on metastasis.** A549 (**Panel D**) or LL-2 (**Panel E**) cells were incubated for 1 hr in control media. The CM was harvested from unstimulated fibroblasts or fibroblasts stimulated with tMVs. Following incubation, A549 cells were injected intravenously into SCID (A549) or C57Bl/6 mice (LL-2) to evaluate the number of A549 cells in lungs (shown as number of human cells/ $10^6$  murine cells) and to assess the number of metastases in lungs (LL2 cells), respectively. Data from four separate experiments are pooled together. \* $p < 0.0001$ .



**Table I**

Murine or human fibroblast were stimulated with tMVs derived from murine LL-2 or human A549 cell line. Sixteen hours later, RNA was extracted and real-time RT-PCR was performed. Data is shown as fold of increase over control unstimulated cells.

|                                | <b>LL-2 tMVs</b> | <b>A549 tMVs</b> |
|--------------------------------|------------------|------------------|
| <b>IL-1</b>                    | 12.2+/-2.8       | 10.2+/-3.5       |
| <b>IL-6</b>                    | 9.6+/-4.8        | 12.8+/-4.1       |
| <b>IL-8</b>                    | not done         | 34.2+/-7.5       |
| <b>IL-11</b>                   | 6.3+/-2.1        | 17.6+/-4         |
| <b>LIF</b>                     | 11.6+/-2.1       | 7.4+/-2.1        |
| <b>OSM</b>                     | 7.4+/-0.1        | 2.3+/-0.5        |
| <b>SDF-1</b>                   | 1.8+/-0.1        | 1.1+/-0.3        |
| <b>HGF</b>                     | 1.4+/-1.3        | 0.7+/-0.02       |
| <b>VEGF</b>                    | 16.2+/-0.3       | 9.3+/-3.8        |
| <b>GM-CSF</b>                  | 2.1+/-0.1        | 1.9+/-1.1        |
| <b>TNF-<math>\alpha</math></b> | 9.6+/-0.5        | 1.3+/-1.5        |
| <b>MMP-2</b>                   | 0.9+/-0.2        | 1.3+/-0.5        |
| <b>MMP-9</b>                   | 4.7+/-0.8        | 3.8+/-1.9        |
| <b>TIMP-1</b>                  | 2.2+/-2.5        | not done         |
| <b>TIMP-2</b>                  | 1.1+/-0.9        | not done         |